END
DATE
FILMED
9-80
DTIC

MICROCOPY RESOLUTION TEST CHART

LEVEL Ⅳ

3ɔ

ADVANCED SILICON MATERIAL DEVELOPMENT FOR LADIR

H. Kimura and O.J. Marsh

Hughes Research Laboratories
3011 Malibu Canyon Road
Malibu, CA 90265

DTIC
ELECTE
JUL 3 0 1980
C

June 1980

Approved for public release; distribution unlimited.

ADA087286

DDC FILE COPY

80 7 28 10

REPORT DOCUMENTATION PAGE		READ INSTRUCTIONS BEFORE COMPLETING FORM
1. REPORT NUMBER	2. GOVT ACCESSION NO. AD-A087286	3. RECIPIENT'S CATALOG NUMBER
4. TITLE (and Subtitle) ADVANCED SILICON MATERIAL DEVELOPMENT FOR LADIR		5. TYPE OF REPORT & PERIOD COVERED Interim Report. 15 Aug 1978 — 15 Aug 1979
		6. PERFORMING ORG. REPORT NUMBER
7. AUTHOR(s) H. Kimura and O.J. Marsh		8. CONTRACT OR GRANT NUMBER(s) F33615-78-C-5062
9. PERFORMING ORGANIZATION NAME AND ADDRESS Hughes Research Laboratories 3011 Malibu Canyon Road Malibu, CA 90265		10. PROGRAM ELEMENT, PROJECT, TASK AREA & WORK UNIT NUMBERS 48
11. CONTROLLING OFFICE NAME AND ADDRESS Air Force Materials Laboratory Air Force Systems Command United States Air Force Wright-Patterson AFB, OH 45433		12. REPORT DATE June 1980
		13. NUMBER OF PAGES 48
14. MONITORING AGENCY NAME & ADDRESS(if different from Controlling Office) Air Force Materials Laboratory Wright-Patterson AFB, OH 45433 Project Engineer: Thomas C. Chandler		15. SECURITY CLASS. (of this report) UNCLASSIFIED
		15a. DECLASSIFICATION DOWNGRADING SCHEDULE

16. DISTRIBUTION STATEMENT (of this Report)

Approved for public release; distribution unlimited.

17. DISTRIBUTION STATEMENT (of the abstract entered in Block 20, if different from Report)

18. SUPPLEMENTARY NOTES

19. KEY WORDS (Continue on reverse side if necessary and identify by block number)

Float-zoned silicon, IR detector material, Gallium-doped silicon, LADIR materials study, Diffusion during growth of Si:Ga

20. ABSTRACT (Continue on reverse side if necessary and identify by block number)

This interim report gives dopant distribution results from several float-zoned <100> silicon crystals. Uniformity of Ga improves as the growth rate is decreased and the rotation rate during growth is increased. The results agree qualitatively with diffusion theory and show promise of substantial uniformity improvement over state of the art Si:Ga material for IR detector applications.

DD FORM 1473 EDITION OF 1 NOV 65 IS OBSOLETE
1 JAN 73

TABLE OF CONTENTS

LIST OF ILLUSTRATIONS

SECTION 1

INTRODUCTION AND SUMMARY

The success of extrinsic Si monolithic focal plane arrays, in which a single chip of Si material incorporates both a high density of IR sensitive detectors and the associated signal-processing circuitry, depends on the availability of Si material with sufficiently uniform IR responsivity. In contrast to detector arrays assembled from discrete components, there is no possibility of selecting or adjusting individual detector elements; uniformity must be built into the extrinsic Si substrate material at the wafer stage of processing. There is a limited possibility of compensating for nonuniformities by off-plane processing, but this is feasible only to the extent that the nonuniformities are small to begin with.

A precise specification of the required degree of uniformity is not yet available, but it is clear that improvements in the state of the art are desirable. The objective of the work reported here is to carry out crystal growth and doping operations in ways that will result in the most nearly uniform distribution of the significant impurities. The emphasis is on Ga-doped Si. In Si:Ga detectors, the Ga concentration affects responsivity through the quantum efficiency; since the detector elements are likely to be fairly thick (say 0.5 mm) along the light path, nonuniformities in Ga concentration on a smaller spatial scale may average out. The concentrations of compensating donors (mostly P) and of B influence the responsivity through their effect on the photoconductive lifetime and hence the photoconductive gain. In the usual operating regime of Si:Ga detectors, the responsivity is proportional to $(N_P - N_B)^{-1}$. To achieve the operating temperature appropriate to Ga-doped Si rather than the much lower temperature necessary for B-dominated material, N_P must exceed N_B. However, the amount by which N_P exceeds N_B should be small enough to provide a high responsivity without being so small that the nonuniformities of P and B separately are large compared to the difference between their concentrations. Unfortunately, the best present-day technology for Si results in an

irreducible residual concentration of B. Although this concentration is small, it constitutes a lower limit for the P concentration.

Like B, P is present in the high-purity polycrystalline Si that is the starting material for high-quality Si crystal growth. It differs from B, however, in that it can be removed by a succession of vacuum float zone operations, so that a crystal can be prepared that is essentially free of P. By means of neutron transmutation doping (NTD), an inherently uniform and precise doping method, P can be reintroduced into the crystal after the final growth step. We have verified on this contract that the distribution of B as a result of growth is quite uniform, so that $N_P - N_B$ can also be uniform. Our strategy, therefore, has been to explore modifications in the growth process to make the Ga distribution as uniform as possible. Our proposed process is to remove P from low-B polycrystalline silicon by successive vacuum zoning, add Ga in a final doping zone pass with growth parameters chosen for optimum Ga uniformity, and add P uniformly by NTD with a dose chosen to achieve a specified value of $N_P - N_B$ in the final material.

During the first year of the program, we emphasized the study of the effect of float zone growth parameter variations on dopant distribution. Four 2-in.-diameter crystals, three Ga-doped and one B-doped, were grown in the <100> direction. In two of the Ga-doped crystals, Z108Ga and Z118Ga, various combinations of growth and rotation rates were tried to examine their effects on the radial Ga distribution. Crystal Z144B is a B-doped crystal grown to assess the uniformity of B distribution. This is important from the standpoint of achieving a low and uniform value of $N_P - N_B$. Crystal Z095Ga is a Ga-doped crystal grown with a cooling ring placed near the growth interface to see if the thermal profile at the interface can be altered sufficiently to improve the uniformity. The uniformity on a microscopic scale was assessed by measuring the spreading resistance across the sample in the radial direction with a Mazur ASR-210 Automatic Spreading Resistance Probe. It was used in the two-probe mode so that the spreading resistances of two contact points separated by a distance of $\sim$400 µm could be measured across the sample. Resistivities of the sample at 5-mm

7

intervals were also measured by the four-point-probe method to give an indication of average doping over a large interval.

The results of the measurements made to date indicate that spatial fluctuations in Ga concentration can be significantly reduced by the proper choice of growth and rotation rates. However, those conditions leading to reduced Ga fluctuations (i.e., a high rotation rate and a low growth rate) are also those under which it is very difficult to maintain single-crystal growth. Therefore, during the next year we will seek an optimization between uniformity and reasonable crystal yields. There is a promising indication that an additional reduction in fluctuation may be achieved by thermal diffusion during a high-temperature annealing process. We plan to explore this diffusion process and its effect on the optimization of the crystal growth process.

To furnish additional background on two technical issues of key importance to the unifomrity of extrinsic silicon detector arrays, we have included two appendices. Appendix A describes the float-zone crystal growth process and briefly discusses the factors that control the uniformity of the gallium concentration in a doped single crystal of Si:Ga. Appendix B presents information obtained prior to this program which shows the beneficial effects of counterdoping by neutron trans-mutation as mentioned above.

SECTION 2

EXPERIMENTATION

A.   SEGREGATION THEORY

Compositional striations result mainly from microscopic growth
rate fluctuations arising from the rotation of the crystal in an
asymmetric thermal field. Other minor variations in composition are due
to unsteady thermal convection flows in the melt.

The steady-state solution to the diffusion equation may be used to
analyze the effects of growth and rotation rate on the composition.
(This solution was originally developed for Czochralski growth.) In
the range over which we can vary the growth and rotation rates, the
rotation rate ω is larger than D/δ^2,

$$\omega > \frac{D}{\delta^2} \quad ,$$

where D is the diffusion coefficient of the solute in liquid, and δ
is the thickness of the interfacial boundary layer. The steady-state
solution to the diffusion equation of the compositional variation can
be written as[1]

$$\frac{\Delta C/C}{\Delta R/R} = (1 - k_o) \frac{R\delta/D}{(2\omega\delta^2/D)^{1/2}} \quad ,$$

where C is the concentration of solute in the crystal, R is the growth
rate, and k_o is the equilibrium distribution coefficient of the solute.
Figure 1 shows the plot of $(\Delta C/C)/(\Delta R/R)$ versus the rotation rate ω for
the three growth rates. It shows that to minimize compositional fluc-
tuation due to growth rate fluctuations one must minimize the growth
rate and maximize the rotation rate.

Aside from the effects on the segregation behavior of the solute,
changes in the growth rate and rotation rate affect the shape of the
growth interface. At the growth interface, the heat of crystallization
is dissipated through the crystal by conduction and from the crystal to

---

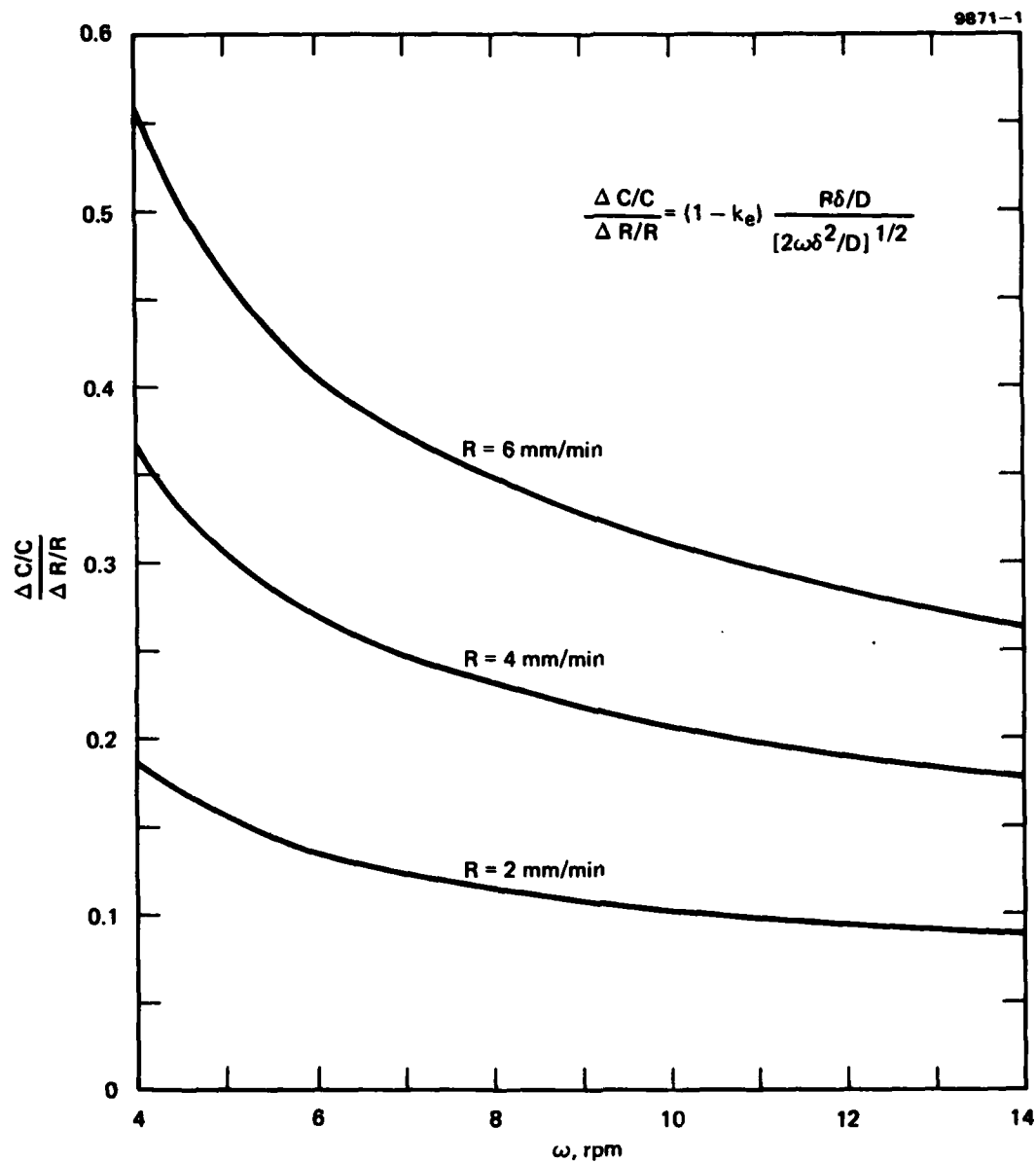[1]D.T.J. Hurle and E. Jakeman, J. Cryst. Growth $\underline{5}$, 227 (1969).

Figure 1. Theoretical dependence of compositional fluctuations on growth rate (R) and rotation rate (ω).

10

the surrounding atmosphere by radiation. Since the shape of the interface conforms to the freezing isotherm, any change in the rate of crystallization causes a corresponding change in the shape of the inter- face. The advancing crystal boundary becomes more convex toward the crystal as the growth rate increases because of an accumulation of heat at the interface.

Another factor that influences the shape of the interface is the rotation rate of the crystal. When the crystal is rotated fast, the centrifugal force exerted on the convection flows increases the temper- ature around the periphery of the crystal and decreases it at the core. Consequently, the core of the crystal advances toward the melt to flat- ten the interface. An optimum combination of growth and rotation rates can be chosen to approach a flat interface.

B. GROWTH AND ROTATION RATE STUDIES

Crystal Z108Ga was grown to study the effect of growth rate and rotation rate on the segregation of Ga, and the role these rates play in determining the shape of the interface. The following combinations of growth rate and rotation rate were used.

Section	1	2	3	4	5
Growth rate, mm/min	4	4	4	2	3
Rotation rate, rpm	6	8	3	3	3

Figure 2 shows the crystal after etching with a striation etch to reveal the shape of the interface. The crystal is cut where the parameters were changed and evaluation wafers were sliced from the other half of the sectioned crystal. The first combination, a growth rate of 4 mm/ min and a rotation rate of 6 rpm, is what we have normally used to grow Ga-doped crystals. Striations start to appear where Ga was initially embedded in the polycrystalline Si charge. The shape of the striation shows that the interface is convex toward the growing crystal at this setting.

In the next section, where the rotation rate was increased to 8 rpm while the growth rate was kept at 4 mm/min, the core of the

11

crystal moves further into the melt, forming a flatter interface. The distance between striations decreases because of the increased rotation rate.

The third section was grown by decreasing the rotation rate to 3 rpm while keeping the growth rate constant at 4 mm/min. As the rotation decreases, the downward velocity component of the convection flow increases to raise the temperature at the center of the crystal. The result is a very pronounced convex profile toward the crystal.

In the last two sections, the growth rate was decreased to 2 mm/min and 3 mm/min. The resulting flattening of the interface appears clearly although not enough time was allowed to reach a steady state.

Spreading resistance measurements were made on these sections in the radial direction. Figure 3 shows the microscopic fluctuation in resistance for the three sections grown at 4 mm/min. The maximum resistance minus the minimum resistance divided by the minimum resistance times 100 in each 800-µm interval along the radial direction is plotted on the ordinate and the radial distance is plotted on the abscissa in normalized increments of 800 µm width. The traverse in this and following figures is made across a diameter of the wafer.
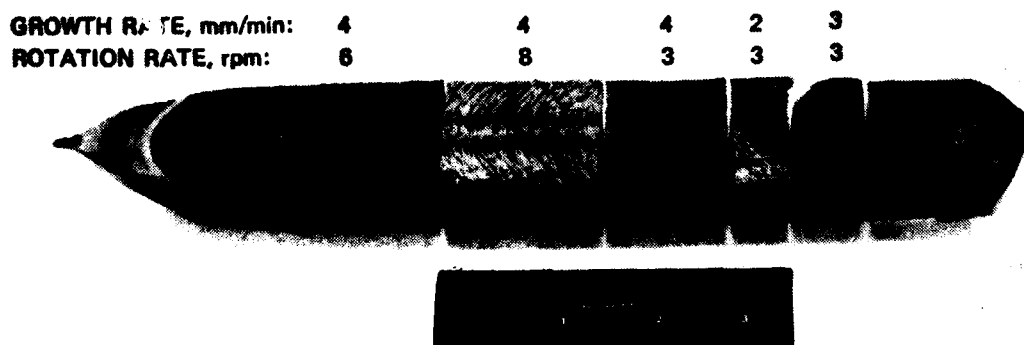

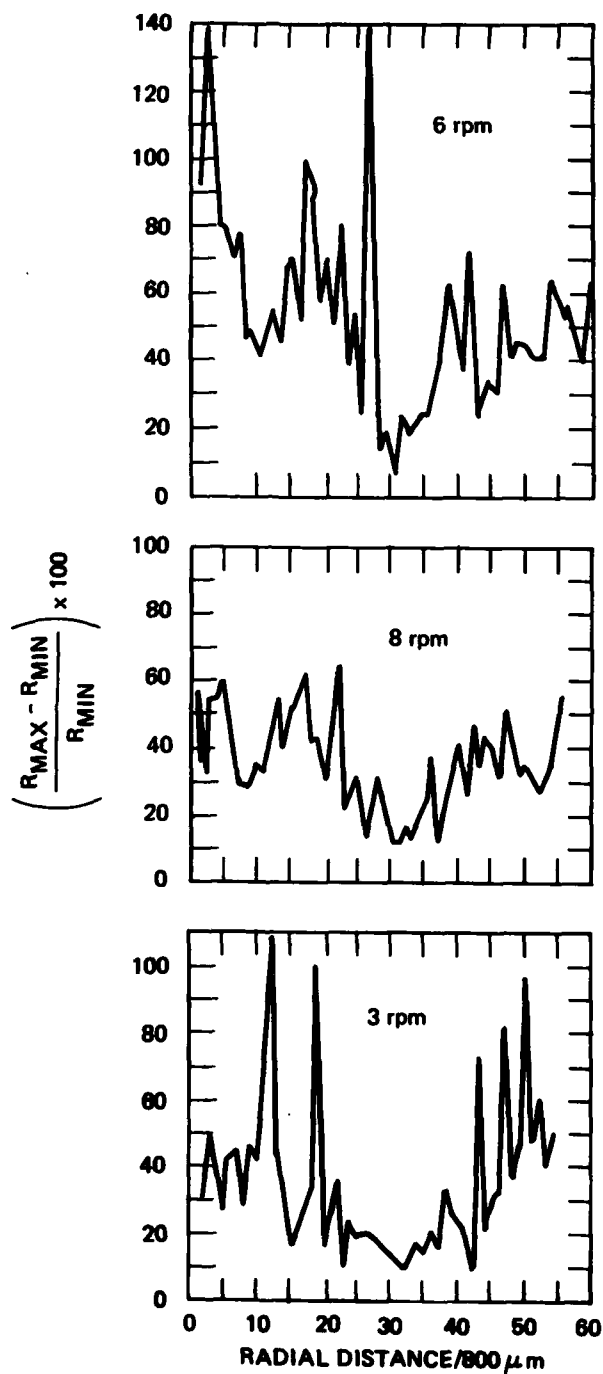Figure 2. The cross section of crystal Z108 Ga etched to reveal the striations in Ga concentration.

Figure 3.
Localized microscopic resistivity fluc-
tuations in Z108 Ga for a growth rate
of 4 mm/hr at three rotation rates
(sections 1, 2, and 3).

13

Comparing the three sections in Figure 3, the uniformity of Ga distribution is clearly worst for the case where the crystal was grown with a 6 rpm rotation ("normal" condition). Comparing the two cases where the crystal was rotated at 8 rpm and 3 rpm, the faster rotation appears to be better. The measurements do indicate, however, that the result is not in agreement with the predictions from the segregation theory or with the shape of the interface. Ambiguity may arise from the two-point-probe spreading resistance measurement, which gives the total value of the two spots separated by the probe separation of 400 µm. Single probe measurements are being planned to resolve the inconsistency.

Figure 4 shows the uniformity in the last two sections of the crystal where the rotation rate was kept constant at 3 rpm but the growth rate was reduced to 2 mm/min and 3 mm/min. We were unable to make a complete scan across the wafer because the crystal cracked (during cutting) in the fourth section, where the growth rate was 2 mm/min. The figure shows that the uniformity is considerably better for the 3 mm/min growth rate. It appears, however, that time allowed to reach a steady state was not sufficient to yield a fair assessment of the effect of a slow growth rate. The uniformity of the last section, grown at 3 mm/min with 3 rpm rotation, appears comparable to that of section two, which was grown at 4 mm/min and 8 rpm rotation. In Figure 5, the average values of the concentration of Ga in 800-µm intervals determined by the spreading resistance measurement are plotted together with the values obtained by the four-point probe measurements. This averaging over 800-µm intervals provides a scale intermediate between that of the direct spreading resistance measurements and that of the four-point probe. The absolute values of concentration do not agree with the four-point probe values because of our use of an uncorrected calibration curve to convert spreading resistance to concentration. Since our interest lies in assessing the fluctuations within a wafer, no effort was made either to recalibrate or to work out a polishing procedure to obtain reproducible spreading resistance values.

14
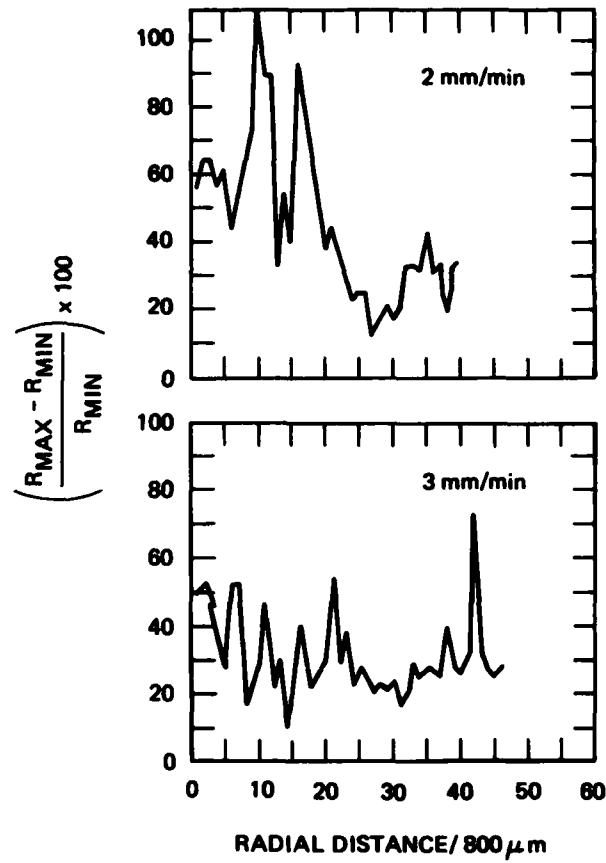
Figure 4.
Microscopic resistivity fluctuations in
Z108 Ga for a rotation rate of 3 rpm and
two relatively slow growth rates
(sections 4 and 5).
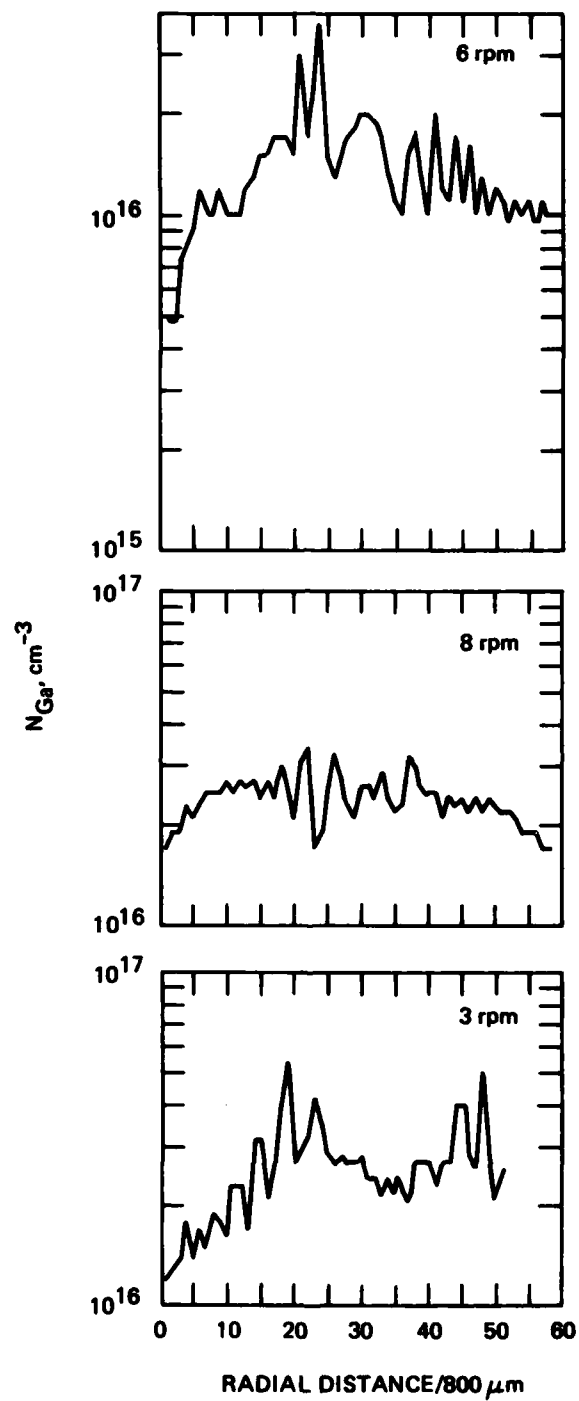
(a)   Section 1, 2, and 3 by spread-
ing resistance technique.

Figure 5.   Ga concentrations in Z108 Ga
in each of the 5 sections.

16
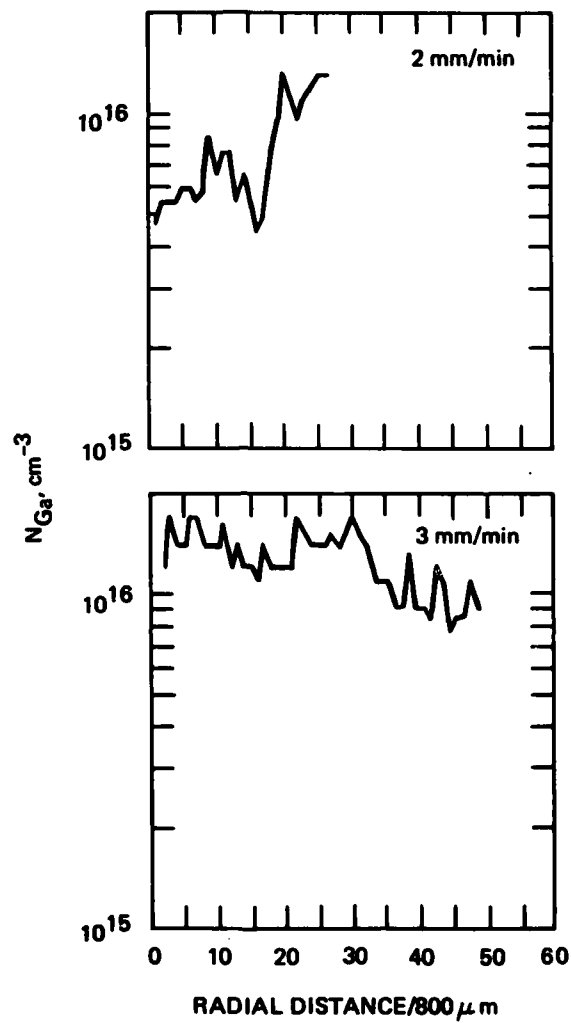
(b) Sections 4 and 5 by spreading
resistance technique.

Figure 5. Continued.
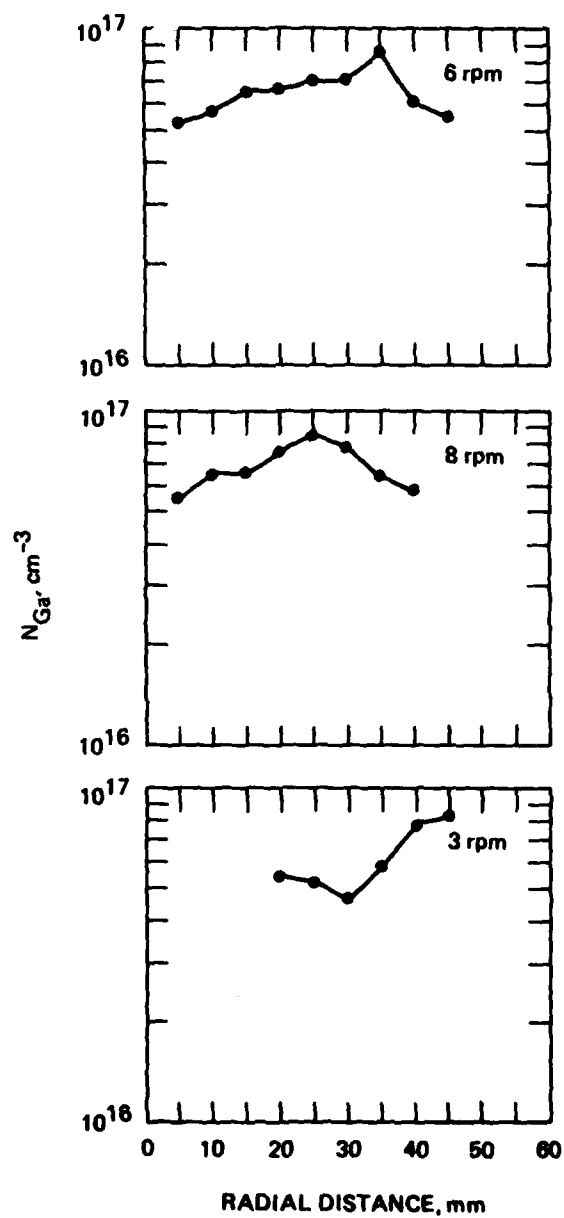
(c) Sections 1, 2, and 3 by four-
point probe method.

Figure 5. Continued.

18
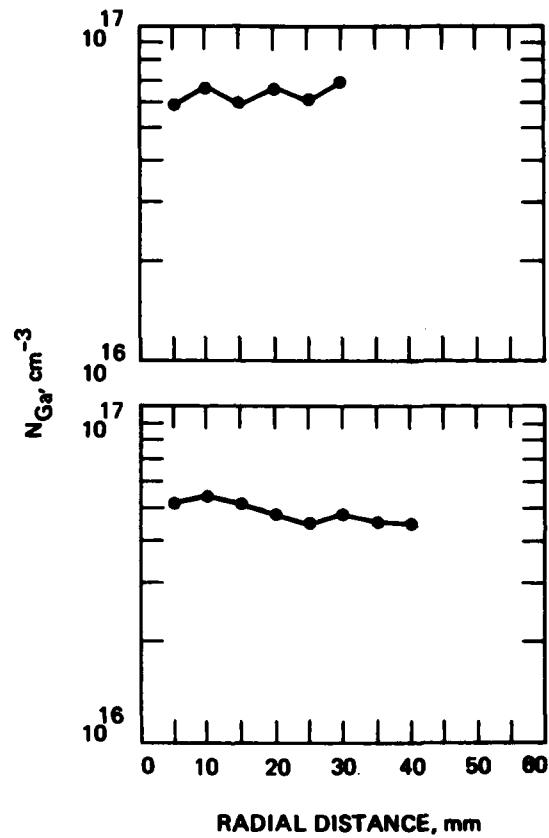
(d) Sections 4 and 5 by four-point
probe method.

Figure 5. Continued.

The mean values, $\overline{X}$, and the associated standard deviations, σ, are tabulated below:

Z108	1	2	3	4	5
$\overline{X}$	53	36	34	46	31
σ	28	14	22	24	13

$$\overline{X} = \frac{\overline{R_{max} - R_{min}}}{R_{min}} \times 100$$

The distributions appear different from the previous plots, where the microscopic fluctuations were plotted against radial distance. The fluctuations in the average concentration are considerably less in the second and fifth sections, where the rotation rate was increased or the growth rate was decreased from the normal values used in Section 1. The lower concentration of Ga near the periphery that usually occurs arises mainly from the thinner interfacial layer, which results from a higher tangential velocity. The mean concentrations from the spreading resistance measurements and the associated standard deviations are tabulated below:

Z108 Ga	1	2	3	4[a]	5
$\overline{N}_{Ga} \times 10^{-16}$, cm^{-3}	1.4	2.4	2.6	0.79	1.3
$\sigma \times 10^{-16}$, cm^{-3}	0.58	0.39	0.88	0.30	0.25

[a]Only 1/2 wafer was available for analysis.

C. UNIFORMITY OF BORON DISTRIBUTION

A B-doped crystal, Z144B, was grown to assess the uniformity of residual B distribution. Since a wafer can be uniformly counter doped with P by neutron transmutation, the uniformity of B distribution is important in achieving a low and uniform value of $N_p - N_B$. A Czochralski-grown crystal doped with 10^{15} cm^{-3} B was used as a starting charge. The crystal was grown at 4 mm/min and rotated at 6 rpm.

20

Figure 6 shows the plot of spreading resistance versus radial distance, and Figure 7 shows the plot of the microscopic fluctuations for Z144B. As expected from the near unity distribution coefficient of B (k_o = 0.8), the uniformity is excellent. The mean value was 17, and the standard deviation of the percent fluctuations in the 800-μm segments was 5.2. The background noise of the instrument corresponds to $\sim$10% fluctuation. The nonuniformity of the B distribution in parts of the wafer, therefore, can be much less than 10%.

Figure 8 shows the concentrations of B along the radial distance as determined by the four-point probe measurements. The uniform concentration seen here confirms the results from spreading resistance evaluation.

D. EFFECT OF ENHANCED ROTATION

The effect of rotation rate and growth rate as predicted by the segregation theory was further investigated. Crystal Z118Ga was grown at the maximum rotation rate and at the slowest growth rate possible for that rotation rate. The growth rate was kept constant at 4 mm/min while the rotation rate was increased from 8 rpm to 13 rpm.

Figure 9 shows the photograph of this crystal after it had been cut longitudinally and striation etched. The transition to 13 rpm is clearly visible by the more closely spaced striations and the bulging at the core of the crystal.

Figure 10 shows the spreading resistance in the radial direction of the two sections in which 8 rpm and 13 rpm rotation rates were used. The correlation between the etched pattern and the spreading resistance scan is shown in Figure 11. Large amplitude fluctuations toward the edges of the wafer correlate with the two probes intersecting the rotational striations. At the core of the wafer, where the interface is flat and almost perpendicular to the growth axis, the spreading resistance profile is flat, showing only small amplitude fluctuations due to unsteady convection flows.
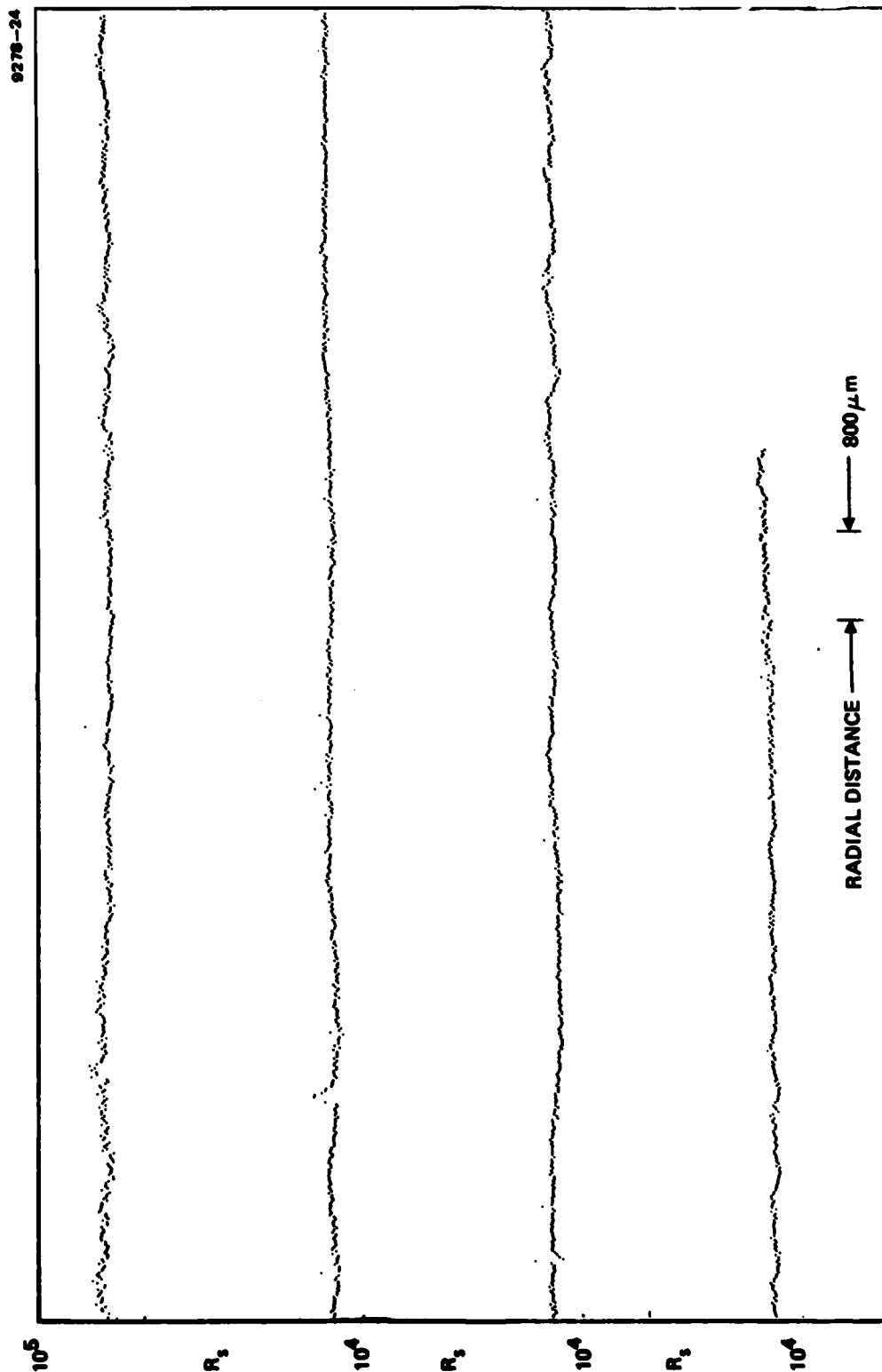
Figure 6. Radial distribution of resistivity in a B-doped crystal (Z144B).
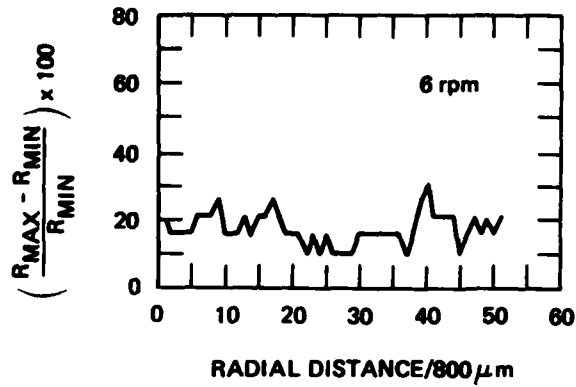
Figure 7.
Localized microscopic
resistivity fluctuations
in Z144B.

Figure 8.
Radial distribution of B in
Z144B as determined by
four-point probe resistivity
measurements.

13 rpm   8 rpm
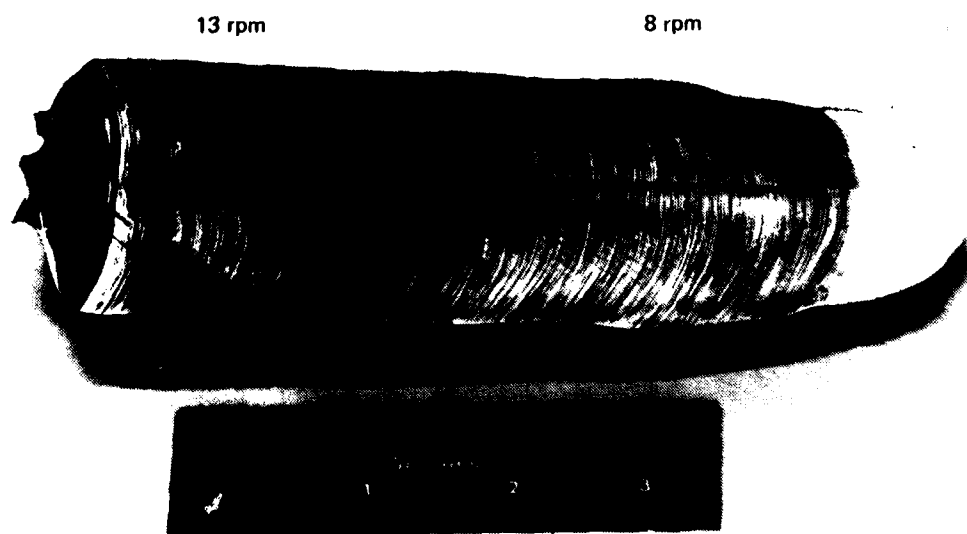
Figure 9.   Cross section of Z118Ga etched to show Ga concentration
striations at two rotation rates.
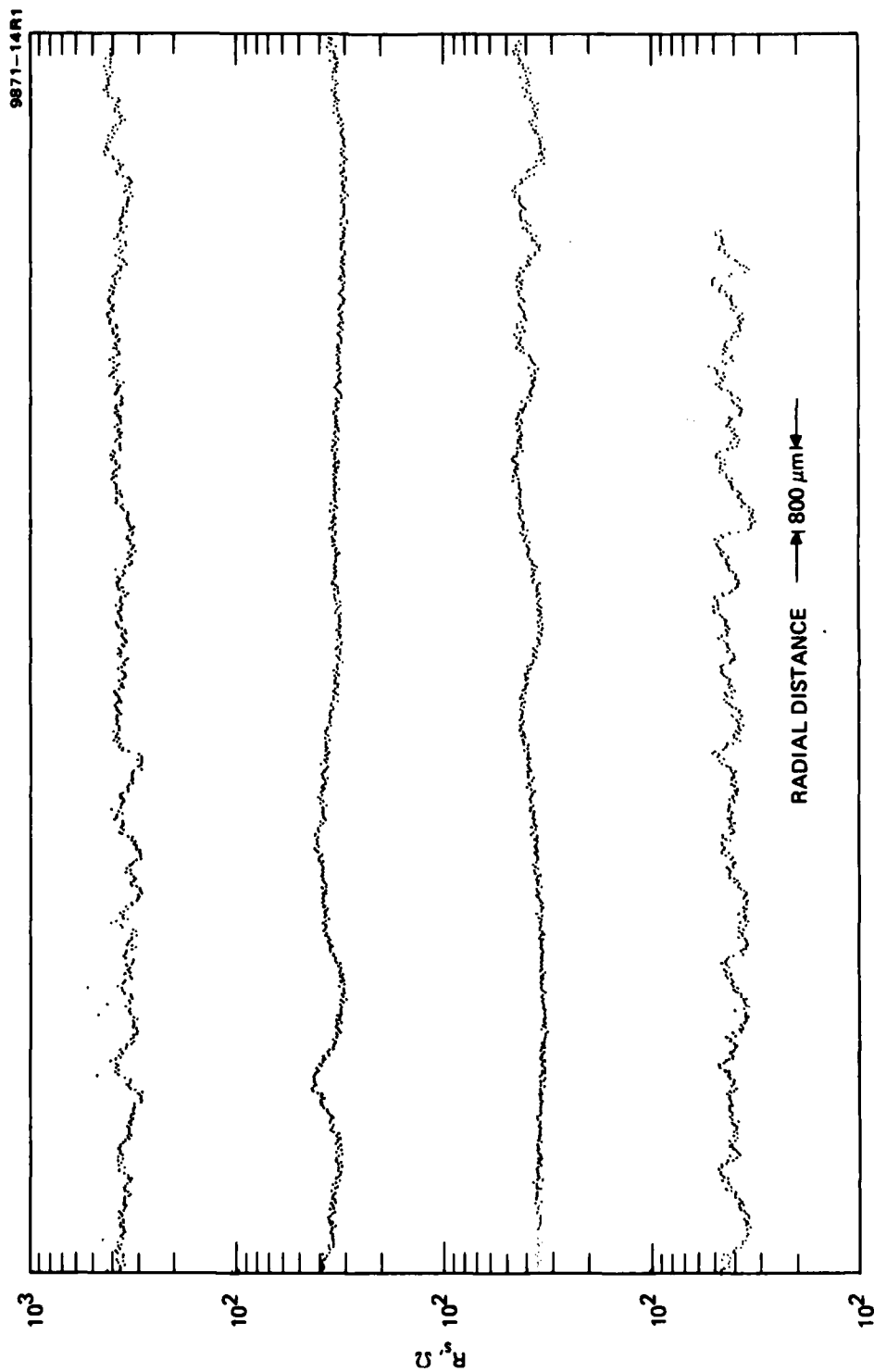
(a) 8 rpm section

Figure 10. Resistivity profile in the radial direction for Z118Ga.
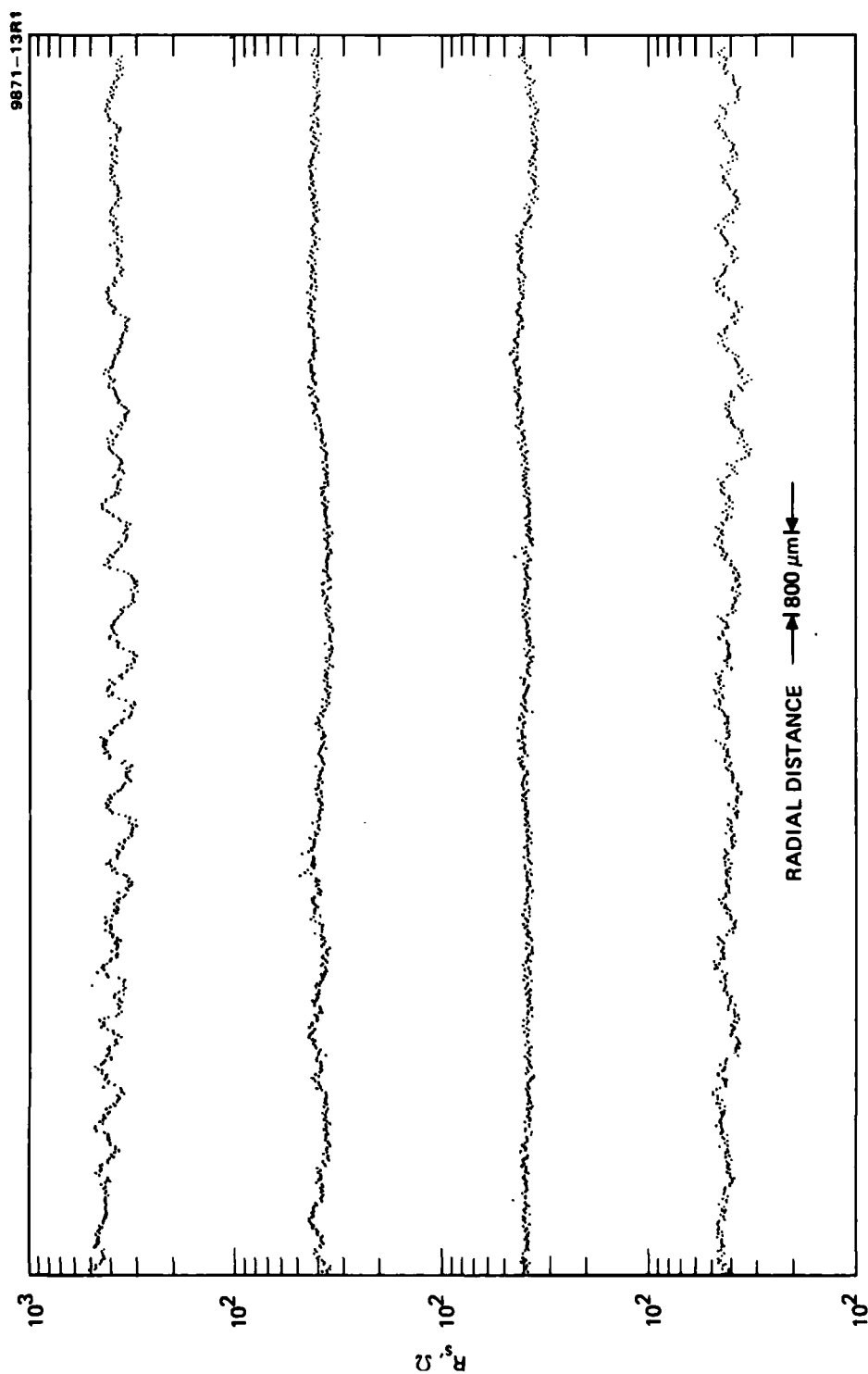
(b) 13 rpm section

Figure 10. Continued.
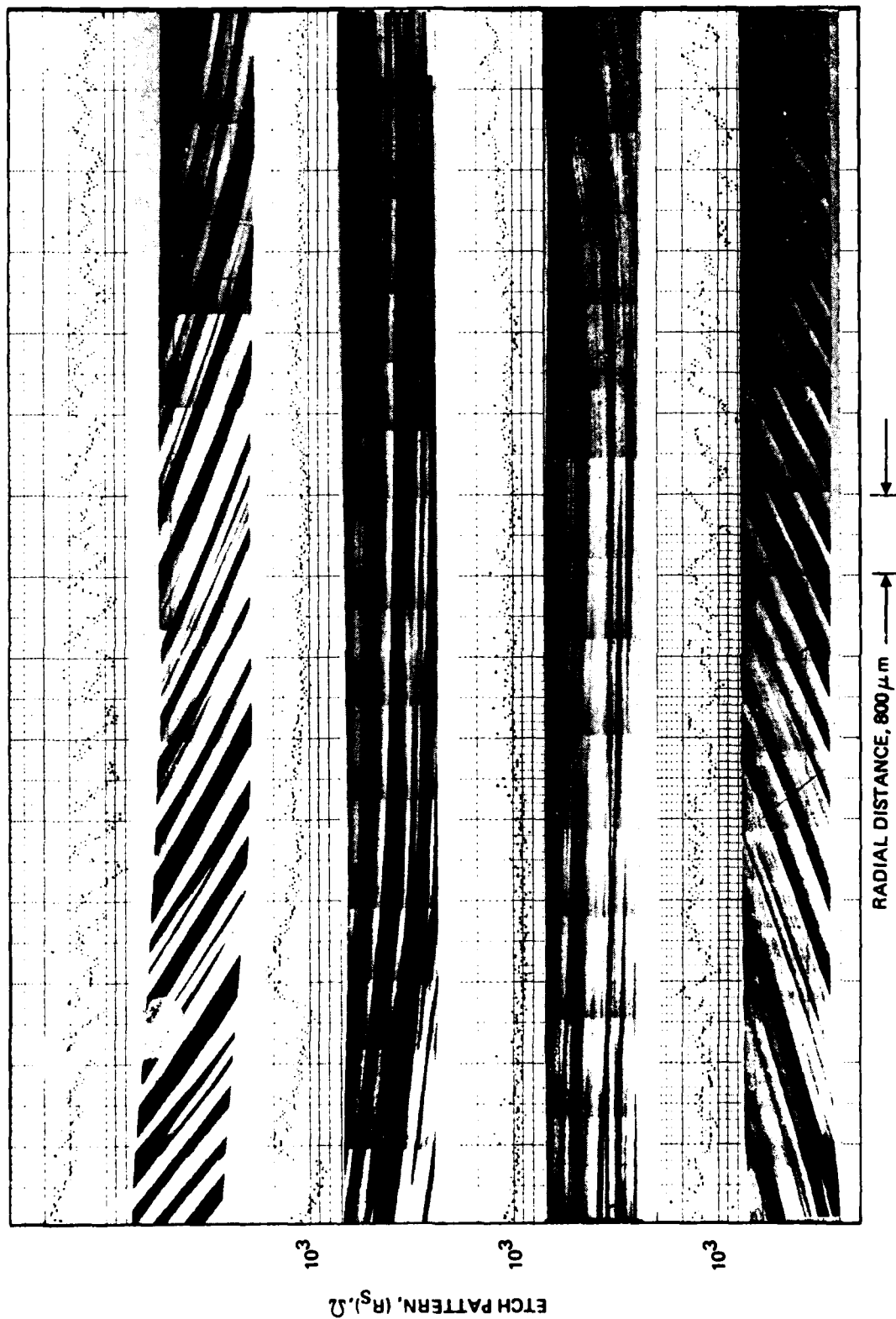
Figure 11. Spatial correlation of etched striation pattern and microscopic resistivity fluctuations for Z118Ga.

27

Figure 12   shows the microscopic fluctuations in the 800-μm segments
along the radial direction. Noticeable improvement is seen in the cen-
tral core region in the part of the crystal rotated at 13 rpm. Although
the mean value of the fluctuations across the diameter is the same, the
13 rpm part appears to have a smaller standard deviation in the central
region as can be seen in Figure 10. The following tabulation shows the
values averaged across the entire diameter.

Z118 Ga	8 rpm	13 rpm
$\bar{x}$	30	30
σ	16	15

The average concentrations in each 800-μm segment along the radial
direction are plotted in Figure 13. The uniformity is about the same
in the two sections. The mean concentration values and the standard
deviations are tabulated below.

Rotation Rate	8	13
$N_{Ga} \times 10^{-16}$, cm^{-3}	4.6	4.7
$\sigma \times 10^{-16}$, cm^{-3}	0.51	0.55

Figure 14 shows the concentration variation measured by the four-point
probe method; it is in good agreement with the data in Figure 13.

E.   EFFECT OF COOLING RING

Since the shape of the freezing interface and therefore the radial
uniformity are governed by the heat balance at the interface, crystal
Z095 Ga was grown with a cooling ring. The cooling ring was placed
∿1 in. below the crystal-to-melt interface and was cooled with Ar
gas. The growth parameters used are given below.

28

Figure 12. Microscopic resistivity
fluctuations for Z118Ga at
two rotation rates.

9871—9
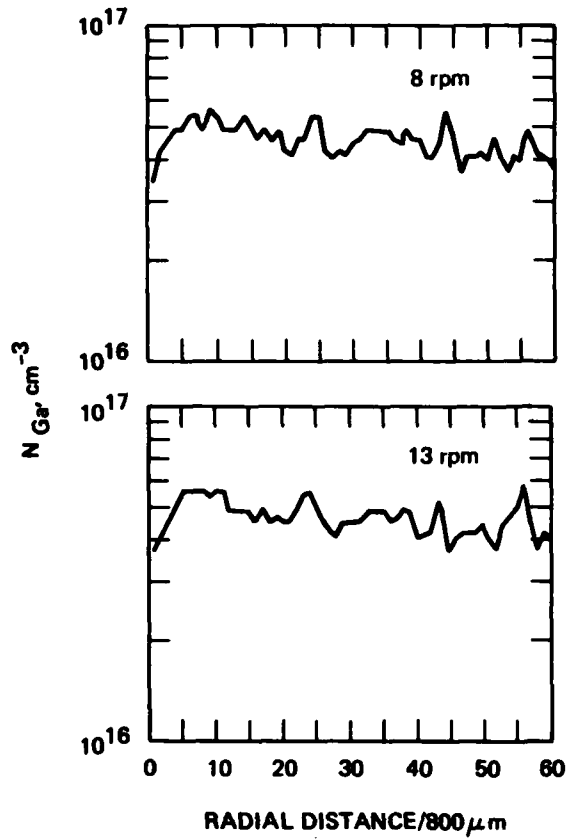
Figure 13.
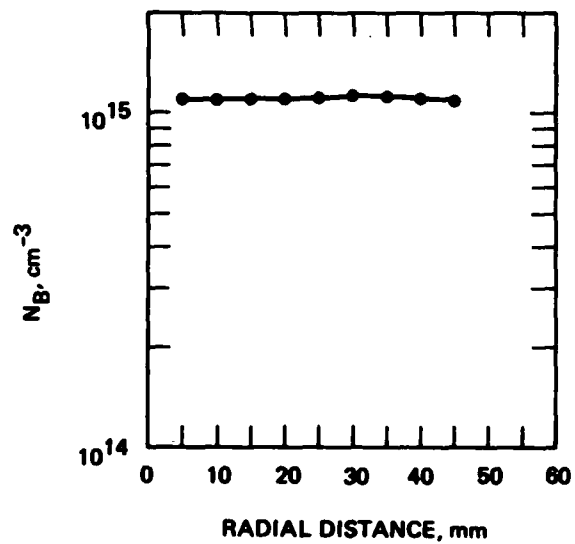Radial distribution of Ga in
Z118Ga for two rotation
rates.

9871—11

Figure 14.
Radial distribution
of Ga in Z118Ga as deter-
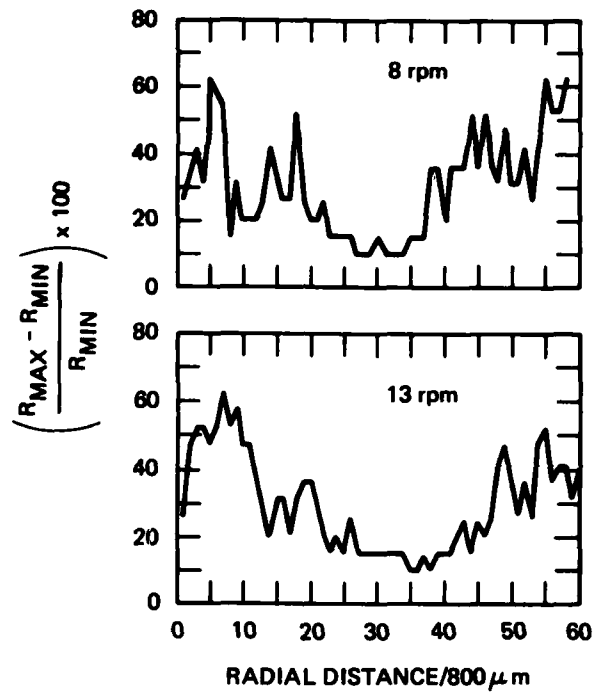mined by four-point probe
resistivity measurements.
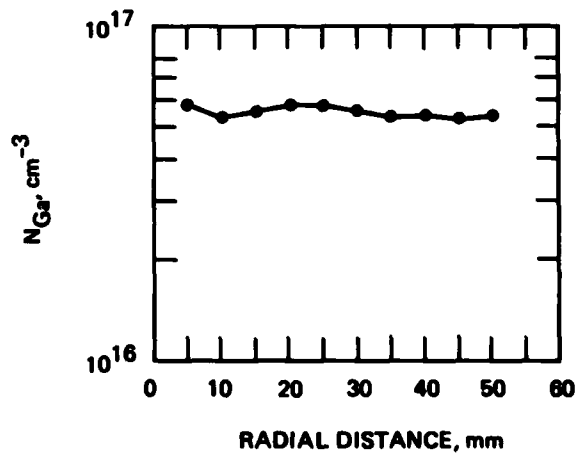
Distance from Seed, cm	Growth Rate, mm/min	Crystal Rotation Rate, rpm
0 to 8	4.2	8.0
8 to 12	4.2	3.3
12 to 19	3.0	3.3
19 to 21	2.5	3.5
21 to 24	2.5	8.0

The spreading resistance profiles and the shapes of the interface show the effect of growth and rotation rates as previously reported, but there was no noticeable improvement due to the cooling ring. No further studies were made on this crystal, and we do not anticipate any more experiments with a cooling ring.

F. THERMAL DIFFUSION

Crystal Z118Ga shows that a good uniformity can be achieved by employing a combination of slow growth rate and fast rotation rates. When the crystal is rotated at 13 rpm and grown at 4 mm/min, the distance between each striation is on the order of 400 to 500 μm. Although a better uniformity might be achieved by changing the coil design, it would require a considerable amount of time to examine various configurations, and such work is beyond the scope of this program.

The length of time it takes to reduce the inhomogeneity of a doped wafer by high-temperature diffusion can be calculated using conventional diffusion theory. When, as a result of crystal rotation, the concentration of a dopant $c(x)$ varies sinusoidally along a growth axis, it can be expressed by

$$c(x) = c_o + c_1 \sin (2\pi x/\lambda) \quad ,$$

where c_1 is the amplitude of rotational striation, c_o the average concentration, λ the distance between rotational striations, and x the distance along the growth axis. The diffusion equation applicable to annealing of the striated crystal then becomes

$$c(x) = c_o + c_1 \sin(2\pi x/\lambda) \exp\left[-(2\pi/\lambda)^2 D(T)t\right]$$

where $D(T)$ is the diffusion coefficient of the impurity, and t is the diffusion time. For Ga in Si at 1300°C, the diffusion coefficient is 4×10^{-11} cm^2/sec. Taking a segment of crystal Z118Ga, which was grown at 4 mm/min using 13 rpm rotation, λ near the edge of the crystal is approximately 480 μm. Calculation shows that for such a crystal the amplitude of rotational striation can be reduced to 64% after annealing at 1300°C for 180 hr. The results of annealing experiments will be included in the final report.

32

SECTION 3

CONCLUSIONS

It is possible to select growth and rotation rates so as to achieve
a flat interface and thus decrease the spatial fluctuations in Ga doping.
The ideal combination would be a higher rotation rate and a smaller
growth rate than we have used so far, if stable growth can be maintained.
In any event, a rotation rate of at least 8 rpm and a growth rate no
greater than 4 mm/min can provide reasonably uniform wafers. We will
employ this combination in the growth of a uniform-responsivity crystal
in the second year of the program.

33

APPENDIX A

FLOAT-ZONE CRYSTAL GROWTH

The float-zone (FZ) process for making crystals starts with a
high-purity rod of polycrystal silicon and involves several process
steps; these steps are modified according to the desired crystal
properties. The quality of the polycrystal rod is the ultimate limita-
tion on the final purity of the crystal. The polycrystal material used
in growing Si:Ga material is a "specialty grade" silicon polycrystal zone-
rod that is selected for its high purity and has a boron concentration
of less than $5 \times 10^{12}/cm^3$.

The FZ processing steps are described in Table A-1. Figure A-1
shows the geometry of the molten zone which is passed through the poly-
crystal rod to remove impurities. On the final crystal doping pass,
a small predetermined mass of Ga is incorporated into the molten zone
to provide a concentration in the melt of about 125 times that desired
in the doped crystal. As the crystal grows, a small portion (0.8%)
of the dissolved Ga is incorporated into the silicon crystal to give
the desired doping level. For IR detector applications, the Ga concen-
tration in the final crystal is about 1 part per million.

The FZ technique for growing 2-in.-diameter $<100>$-oriented Si:Ga,
which we have successfully applied to LADIR material preparation in the
past, is being used in the present program. Our emphasis is on the
choice of growth parameters for the highest possible uniformity. As
explained in the body of this report, the uniformity of the boron dis-
tribution sets the scale of the ultimately achievable uniformity of
responsivity. The lower the average boron content, the more uniform
we expect the final gallium-doped phosphorus-counterdoped silicon to
be (without requiring so much phosphorus counter-doping that the magni-
tude of the responsivity is reduced excessively).

34

Table A-1. FZ Processing Steps

Step No.	Step	Comments
1	Procure high-purity polycrystal rod	N_B and N_p characterized by supplier. These and other properties characterized by HAC from previous growth runs on rods of the same reactor load (of eight-half-rods).
2	Prepurification of polycrystal rod by zoning	Homogenize the polycrystal rod grain structure, remove deep level impurities, and partially remove P by two or more passes in gas or vacuum.
3	Control P counter-doping by partial removal	With polycrystal lots selected for exact initial N_B and N_p, two or or three passes in argon can provide the desired N_p/N_B ratio.
4	Ga seed doping	This is a reproducible, reliable method if the molten zone volume is kept constant and the same zoning conditions are used on each doped crystal.
5	Dislocation-free single-crystal growth, $\langle 100 \rangle$ orientation	Must be done in one pass.
6	Evaluate	
7	Fabricate the polished wafer	

5892

35

POLYCRYSTAL
ROD

R.F. ZONING
COIL

MOLTEN ZONE

[100]
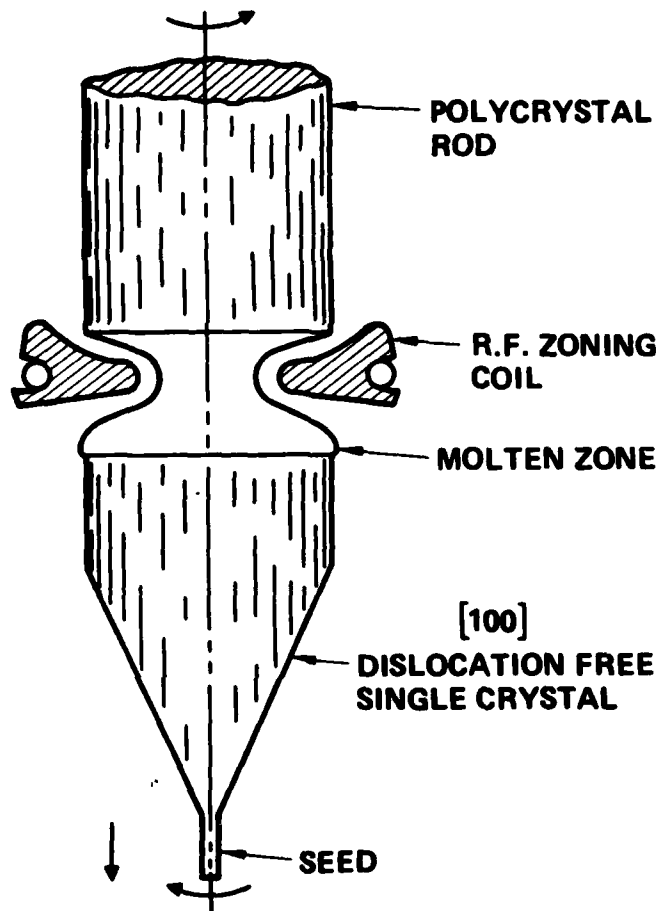DISLOCATION FREE
SINGLE CRYSTAL

SEED

Figure A-1. Geometry of the float-zone crystal
growth process.

The key factors in reducing the nonuniformity of dopant distribution are the planarity of the growth interface and the thermal symmetry of the growth system. We are adjusting the growth parameters to optimize these factors, working first with the gallium distribution to monitor the success of the adjustments. Gallium, with a distribution coefficient much less than unity, is much more sensitive to the factors causing nonuniformity than phosphorus or boron. We use spreading resistance measurements, striation etching, and Hall-effect measurements to assess the uniformity.

Various growth parameters affecting the shape of the freezing interface, the boundary-layer thickness, the thermal convection flows, and therefore the long- and short-range uniformity in FZ growth have been extensively examined by Keller.* We are following his classification in investigating the effects of the following growth parameters:

- External zone length
- Seed rotation
- Feed rod rotation
- Eccentric rotation of freezing interface
- Eccentric rotation of melting interface
- RF coil design
- Growth rate.

A. EXTERNAL ZONE LENGTH

The external zone length can be varied by stretching or squeezing the molten zone, although the range of variation is limited by melt stability requirements for a 2-in.-diameter crystal. A long external zone length leads to poor electrical coupling between the coil and the

_____

*W. Keller, J. of Crystal Growth **36**, 215-231 (1976).

melt and, consequently, to small rf field and temperature gradients at the melt surface. As a result, the external zone length is large compared to the small internal zone length with a bulging crystal interface toward the melt. Consequently, the radial uniformity is poor, giving a concentration profile that is high at the center of the crystal. With the proper combination of growth and rotation rates, a short melt zone having equal internal and external lengths has been found to give the best uniformity.

B. SEED ROTATION

Rotation of the growing crystal plays an important role in determining the thickness of the interface boundary layers adjacent to the crystal and the shape of the interface. Although rapid seed rotation is advantageous in that it leads to a thinner boundary layer where the depletion of the accumulated solute atoms depends only on diffusion, the combination of centrifugal force and the thermal convection pattern causes the central portion of the freezing interface to bulge. The optimum rotation rate is dependent on the crystal orientation, the melt zone length, and the growth rate.

C. FEED-ROD ROTATION

The effect of increasing feed-rod rotation on the growing interface is similar to that of the seed rotation; increasing rotation rate decreases the internal zone length and causes the growing interface to bulge. Counter-rotation of the crystal and feed rod generally gives a smoother profile with better reproducibility, which may be due to better stirring action.

D. ECCENTRIC ROTATION OF FREEZING INTERFACE

Eccentric rotation of the crystal can be obtained by moving the crystal several millimeters to the side from where it would be for concentric rotation. With eccentric rotation, the convection flows are no longer symmetric, which prevents the colder currents from flowing toward

the center and prevents the center of the crystal from bulging. Eccentric rotation leads to nonstationary convection flows because of the rotation in an exaggerated asymmetric thermal field, which promotes better mixing but causes increased microscopic fluctuations.

Asymmetric thermal fields cause all crystals to have rotational striations, which results in large macroscopic concentration variations of the dopant and other impurities. Eccentric rotation may find its rotational axis coinciding with the thermal center, thereby eliminating the melt-back and the major growth rate fluctuations caused by rotation. The degree of eccentricity that yields the best uniformity must be sought for the particular rf coil used.

E. ECCENTRIC ROTATION OF MELTING INTERFACE

Eccentric rotation of the feed-rod must certainly play a role in determining the flow pattern, and therefore, the shape of the freezing interface. Variations of the eccentricity may offset the thermal asymmetry and improve the uniformity.

F. RF COIL DESIGN

The inner coil diameter and the contours (height, inner tapering, stepping) are important in determining the melt shape, (i.e., the external and internal zone lengths). A small internal diameter leads to good rf coupling and a stable molten zone with little tendency toward spill-over and freeze-out in the center.

Although it is not directly related to coil design, the installation of an after-cooling ring or a heater below the coil should offer additional flexibility in shaping the freezing interface. It may enable us to control the cooling rate of the crystal while it is in the plastic state; this is an important parameter in reducing the crystal strain. However, initial experiments with a cooling ring have not been encouraging.

G. GROWTH RATE

Essentially, two growth rates are operating simultaneously during growth, one is the lowering rate of the growing crystal or the feed rod, and the other is the microscopic growth rate. Since the latter arises from transients in the melt, it is more difficult to control. The lowering rate, however, is set by the crystal grower and is dependent on the nature of the dopant and other impurities. In conjunction with other growth parameters, the following factors are affected by the lowering rate:

- Interface shape

- Dopant segregation

- Dopant density.

The interface shape is sensitively affected by the lowering rate because of its effect on the steady-state heat balance. When the heat of crystallization is not efficiently dissipated by radiation and conduction, the center of the crystal becomes hot with respect to the periphery of the melt, and the freezing interface becomes concave. The ideal interface shape (from the standpoint of radial dopant uniformity) is a flat interface. The optimum combination of lowering rate with the rotation rate must be determined experimentally.

Dopant segregation is another factor that is affected by the lowering rate because of the dependence of growth rate on the effective distribution coefficient. The effective distribution coefficient increases with growth rate because of the pile-up of dopant atoms in the boundary layer. The depletion of the dopant from the melt will be faster, the faster the growth rate, which will enhance axial nonuniformity.

The convection flows also are affected by the growth rate. A high growth rate increases the temperature differential between the surface and the center of the melt, thereby increasing the driving force for the thermocapillary flow. The flow can become oscillatory and produce striations.

APPENDIX B

USE OF NEUTRON TRANSMUTATION DOPING TO IMPROVE UNIFORMITY

### A. UNIFORMITY OF RESPONSIVITY

An important materials property that has received little previous attention is the uniformity of the distribution of the three major dopants: Ga, B, and donors (P). Their spatial variations in concentration relative to each other directly affect the local detector responsivity and, if the variations are sufficiently large, also the achievable dynamic range of a monolithic focal plane array (MFPA).

Variations in the Ga concentration from detector to detector in the MFPA directly affect IR absorption and therefore the response from detector to detector. Equally important is the uniformity of the net compensation, $N_D - N_B$. A spatial variation in net compensation causes a nonuniformity in carrier lifetime and thus in responsivity. When a detector is operated near the peak of the η versus αd curve, the effect of N_{Ga} variations is minimized, and the $N_D - N_B$ variations become the dominant nonuniformity effect.

Spot scans of detector responsivity can be made to reveal nonuniformity. This technique can be used on Si:Ga material to study the uniformity without waiting for processed MPFAs. Figure B-1 shows the concept of this technique.

The scan system consists of a chopped 500K blackbody source with a movable focusing lens and the detector sample mounted in a variable temperature dewar. The focused spot is scanned across the face of the detector; position information obtained from piezoelectric transducers and the signal output from a lock-in amplifier are plotted on an X-Y recorder, as shown in Figure B-2. Nonuniformities are clearly evident. The bottom trace indicates that the spot was below the sample. The next traces slant upward, indicating that the edge of the sample was not parallel to the horizontal scan line. The variations in the upper left and lower right appear to be due to growth striations.

6616-7

0.47 mm

V_B

HALL SAMPLES

SCAN

5.3 mm

hν

1.0 mm
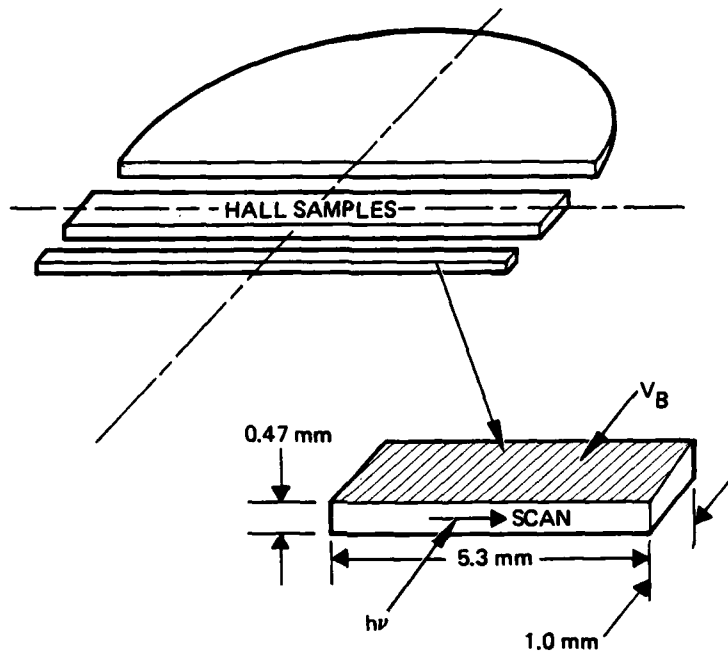
CHOPPED 500 K BLACKBODY SOURCE
FOCUSED TO ~ 30 μm
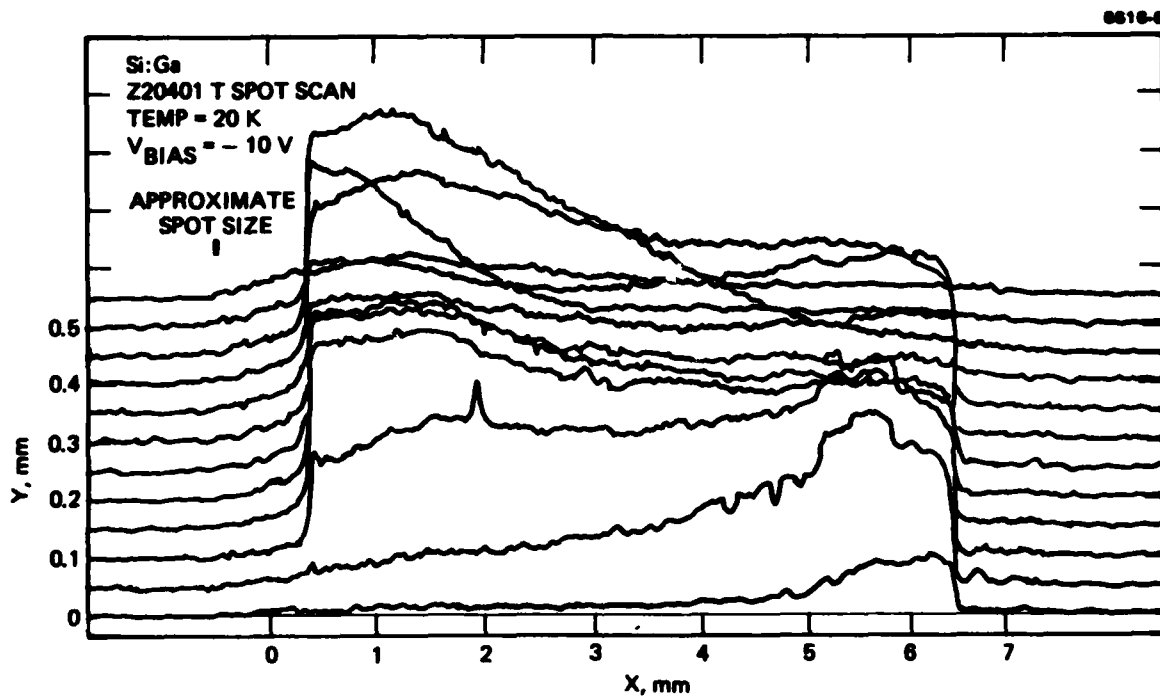
Figure B-1. Si:Ga uniformity test sample.

42

Figure B-2. Spot scans of detector uniformity.

B. PHOSPHORUS COUNTER-DOPING BY NEUTRON TRANSMUTATION IN Si:Ga

An attractive alternative to the conventional method of preparing Si:Ga for MFPA use is to provide the necessary P counter-doping by neutron transmutation of Si-30 after crystal growth. In a thermal neutron flux, each of the 3 natural isotopes of Si (mass number 28, 29, and 30) can capture a neutron and thus increase its mass number by one unit. Only the Si-31 from the Si-30 (natural abundance = 3.12%) is unstable and decays with a half life of 2.62 hr to the stable isotope P-31. Because the capture cross sections for all the Si isotopes are small (<0.3 barns), the thermal neutron flux is not appreciably altered and the capture probability is uniform throughout even a large crystal. Thus the production of P-31 atoms occurs uniformly within the crystal. A subsequent thermal annealing process is used to remove structural damage to the crystal caused by neutron bombardment and silicon recoils. In principle, a crystal is grown "free" of P, its boron content is evaluated by Hall measurements, and neutron irradiation is applied to produce the desired amount of P. The resulting uniformity of the "phosphorus minus boron" distribution should be determined primarily by the uniformity of the boron distribution. Our experience suggests that this simple picture is essentially correct. Detector structures have been fabricated from neutron transmutation counter-doped Si:Ga and tested with excellent results. Figure B-3 shows the improvement in uniformity of responsivity obtained by neutron transmutation doping.

The neutron irradiations are performed under the direction of Dr. Ron Hart at the Nuclear Science Center at Texas A&M. HRL has set up an IR&D program there to study transmutation in silicon. Studies are being made of the spatial distribution and energy distribution of the neutron flux in that part of the Nuclear Science Center's reactor used for Si transmutation. A comparison has been made of electrically active P obtained versus Si-31 activity observed in irradiated samples. These studies have allowed reliable control of the added P concentration and uniformity for application to extrinsic Si IR detector programs. The nature of the damage produced by irradiation is being investigated and
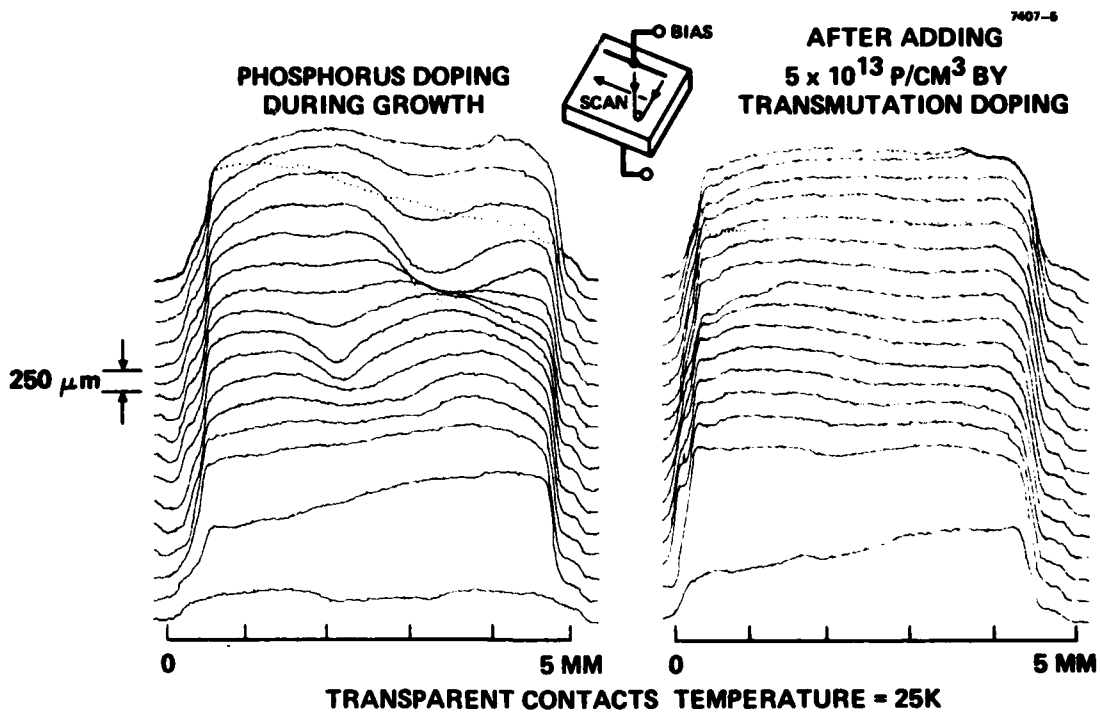
44

Figure B-3. Comparison of responsivity for P-doped Si for conventional growth doping and for neutron transmutation doping.

anneal studies are continuing at HRL to determine optimum annealing procedures.

The data presented in Figure B-4 illustrate the effect of neutron transmutation doping on the low-temperature electrical properties of a Si:Ga sample. Before irradiation, the sample was slightly undercompensated ($N_{boron} \gtrsim N_{donor}$). Irradiation conditions were set to overcompensate the boron by approximately a factor of six. After irradiation and annealing, the full slope of Ga (~ 0.072 eV) appears at the lowest temperatures rather than the shallower slope of the incompletely compensated sample.

Qualitative evidence that the low-temperature electrical uniformity of the Si:Ga is improved by transmutation counter-doping is presented in Figure B-5. The resistance ratio illustrated in the figure is plotted versus 1000/T. Non-uniform doping of the Hall sample causes variations in the rate of carrier freeze-out spatially over the sample. At the lowest temperatures, nonuniformity in the "donor minus boron" concentration dominates the behavior. The result is a temperature-dependent resistance ratio for the two geometrically different, four-terminal configurations used in the Van der Pauw resistivity measurement. Two transmutation-counterdoped samples are shown (one annealed at 850°C for 1 hr and the other at 1000°C for 1 hr) along with a typical conventionally doped Si:Ga sample. Full scale on the R_{12}/R_{34} axis represents a 10% variation in the ratio. The result for the sample annealed at 1000°C is encouraging because it indicates that it is possible to maintain good uniformity during high-temperature processing. This particular sample was "gettered" using a heavily damaged Ar-implanted layer on one surface.
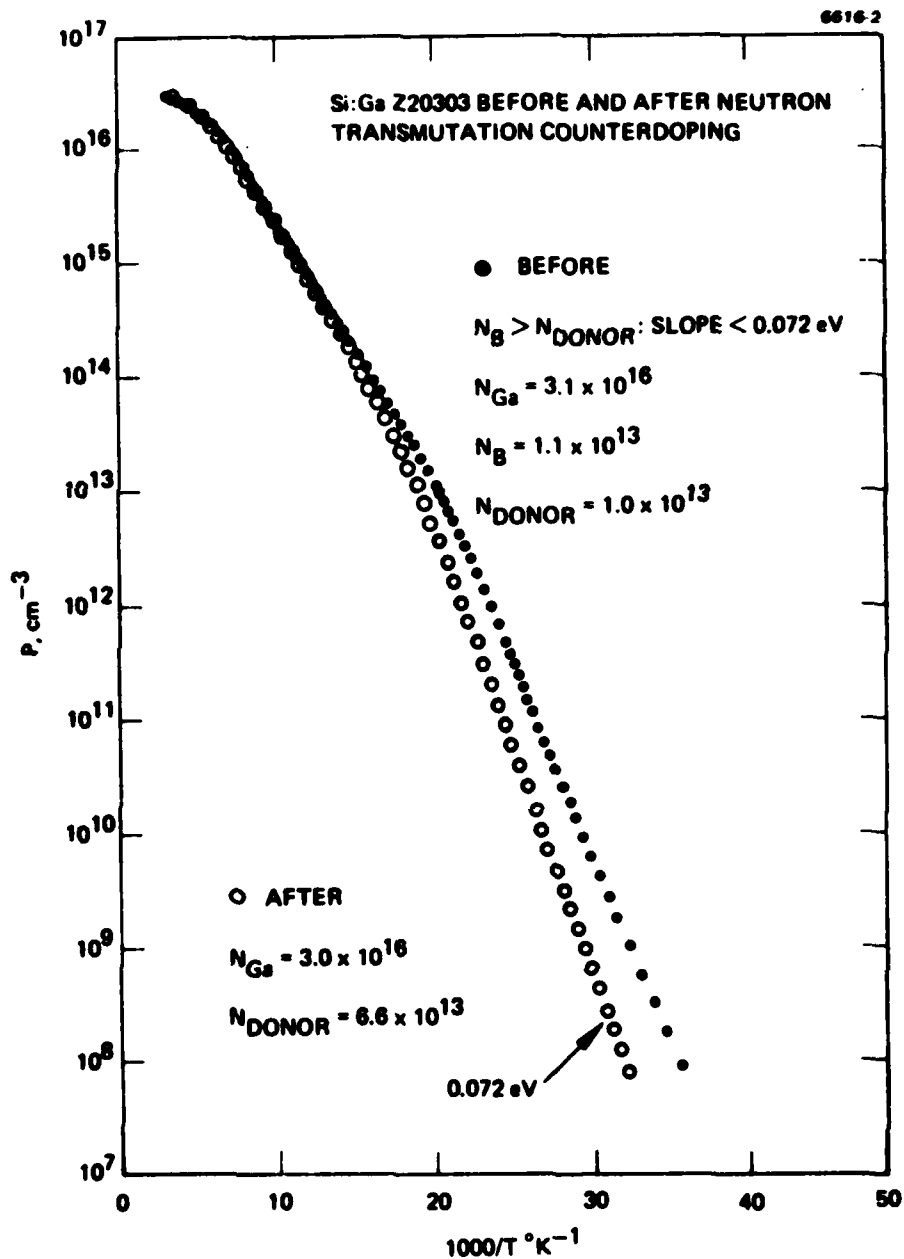
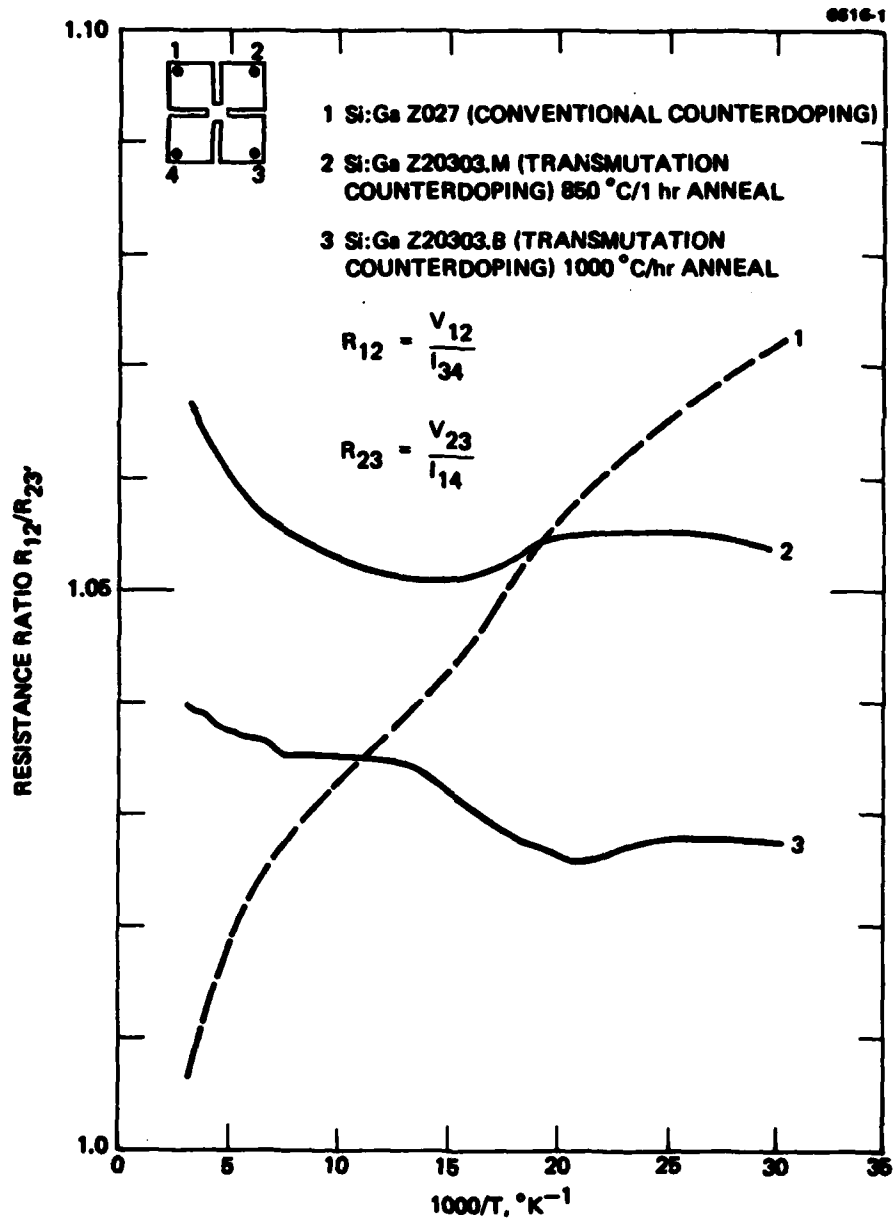Figure B-4.   Si:Ga before and after neutron transmutation counterdoping.

Figure B-5. Plots of resistance ratio, showing uniformity of doping in transmuted material.